Comparison of the Membrane-Bound States of Two Structurally Similar δ-Selective Opioid Peptides by Transferred Nuclear Overhauser Effect Spectroscopy and Molecular Modeling†

Terry O. Matsunaga, Nathan Collins, Varadarajan Ramaswami, Susan H. Yamamura, David F. O'Brien, and Victor J. Hruby*

Department of Chemistry, University of Arizona, Tucson, Arizona 85721

Received January 11, 1993; Revised Manuscript Received September 29, 1993®

ABSTRACT: NMR spectroscopic, peptide–membrane conformational studies on [D-Pen^2, D-Pen^5]-enkephalin (DPDPE), an opioid receptor selective peptide, and an acyclic analog of DPDPE (DPDPE reduced at the disulfide bond) were conducted. The NMR method of transferred nuclear Overhauser effect (TRNOE) was used to obtain NOE profiles of the free and membrane bound forms of DPDPE and acyclic DPDPE. After comparison of the profiles of both peptides in the free and membrane-bound states, we hypothesize that the cyclic DPDPE undergoes little if any conformational change upon interaction with the membrane. However, for the acyclic analog, large changes in the NOE profile associated with backbone and side-chain groups were observed after interaction with the membrane. Results of computerized molecular modeling studies also were consistent with our theory that the free and membrane-bound forms of cyclic DPDPE have very similar free and membrane-bound states. The free acyclic DPDPE has a reverse turn conformation with sidechains situated so that hydrophobic surface exposure to aqueous solution is minimized. After membrane interaction, the acyclic DPDPE has an extended conformation near the carboxy terminus with aromatic sidechains widely separated. We propose that the interaction of the acyclic DPDPE with the membrane surface is mediated by the amino terminus. We further propose that the interaction of the cyclic DPDPE with the membrane surface is limited because the D-Pen^2 side chain is covalently bonded and the aromatic side chains and backbone are only slightly altered after membrane contact. Permeability studies by Ramaswami et al. [(1992) *Biochim. Biophys. Acta 1109*(2), 195–202] demonstrated that the acyclic DPDPE permeated through membranes at a rate 4 times greater than cyclic DPDPE. We conclude that conformational and topographical flexibility may be critical factors in peptide–membrane interactions and permeability of bilayer membranes to opioid peptides.

Opioid peptides interact with a variety of receptors, of which the μ, δ, and κ are the most widely accepted (Hruby & Gehrig, 1989). Over the past decade, major efforts have been directed toward the design of peptides that are receptor selective. However, in the development of peptides for pharmaceutical purposes, receptor selectivity is but one property to consider. Bioavailability, stability, pharmacokinetics, and pharmacodynamics are some of the other factors involved. Recently, our focus has turned to the question of peptide permeability through model bilayer membrane systems as a prototype for studies with biological membranes: in particular, the blood–brain barrier.

Our laboratory has been extensively involved in the design of δ-receptor selective peptide ligands. Because of our interest in studying receptor topography, conformational constraints (Hruby, 1982) are utilized so that we may study ligands that possess only a limited number of conformations. This method was used in designing and synthesizing [D-Pen^2, D-Pen^5] enkephalin (DPDPE)[1] (Mosberg et al., 1983), one of the most highly potent and selective of the δ-receptor selective peptides. Cyclization and the incorporation of the D-penicillamine amino acids completely stabilizes the molecule against enzymatic degradation (Weber et al., 1991, 1992). Having a compound that is highly potent, receptor selective, and biologically stable, we wished to address the question of peptide permeability through biological membranes.

Two aspects of membrane permeability need to be considered; facilitated and passive transport. Although many molecules are actively transported through biological membranes (i.e. glucose), passive diffusion through membranes exists as well (i.e. barbiturates, penicillins) (Banks & Kastin, 1985). It was necessary to first develop and study a model membrane system.

We have undertaken a comprehensive study of peptide permeability through model membranes. Our goal is to study the effects of peptide-membrane interactions via observance of (1) membrane perturbation by differential scanning calorimetry, (2) membrane permeability, (3) peptide penetration into membranes via use of fluorescence quenching spectroscopy, and (4) peptide conformational effects at the membrane surfaces by use of the transferred nuclear Overhauser effect (TRNOE), NMR spectroscopy. The first three components of our design have been addressed elsewhere (Ramaswami et al., 1992; Ramaswami et al., manuscript in preparation). For this study, TRNOE NMR is used to

* To whom correspondence should be addressed.

† This work was supported by a grant from the National Institute on Drug Abuse (NIDA) DA 06284 (V.J.H, D.F.O.). T.O.M. wishes to acknowledge the generous support of the National Institute on Drug Abuse in the form of a NIDA post-doctoral research fellowship, DA 0537102.

® Abstract published in *Advance ACS Abstracts,* November 15, 1993.

[1] Abbreviations: NMR, nuclear magnetic resonance spectroscopy; TRNOE, transferred nuclear Overhauser enhanced spectroscopy; DPDPE, [D-Pen^2, D-Pen^5]-enkephalin; DMPC, 1,2 dimyristoyl-3-*sn*-glycerophosphatidylcholine; NOE, nuclear Overhauser effect; NOESY, nuclear Overhauser effect spectroscopy; COSY, *J*-correlated spectroscopy.

0006-2960/93/0432-13180$04.00/0

characterize peptide interactions with model membranes. Previous work by Milon et al. (1990) addressed the relationship between peptide-membrane interactions and the biological activity of opioid peptides. Their results indicated that Leu-enkephalin, [D-Ala^2, Leu^5]-enkephalin, and [D-Ala^2, Leu^5]-enkephalinamide all adopted a type II′ β-turn around Gly^3–Phe^4 and a γ turn around Gly^2 or (D-Ala^2) at the surface of mixed DOPC–DOPS membranes. The authors concluded that the conformational changes associated with the peptide–membrane interaction was related to their biological activity. Our present work addresses the question of whether or not a peptide conformational change at the membrane surface correlates with rates of peptide interaction and permeability through model bilayer membranes.

The method of transferred NOE NMR spectroscopy (TRNOE) (Clore & Gronenborn, 1982, 1983) allows observation of a bound ligand as it transfers cross-relaxation to the free state, if the rate of chemical exchange is reasonably rapid relative to the spin-lattice (T_1) relaxation of the free ligand. In addition, for a small peptide (MW <1000) in aqueous solvent, the free and bound states exist in two different regimes, namely $\omega\tau_c < 1$ (free) and $\omega\tau_c > 1$ (bound). Thus, the cross-relaxation rates of a small peptide in the free and bound state are of opposite sign, such that the NOEs in the free state are positive while those in the bound state are negative. These can be clearly identified in the phase-sensitive 2D NOESY spectrum since the NOEs are on opposite sides of the spectrum; the positive NOE off-diagonal elements reside on the opposite side as the diagonal whereas the negative NOE off-diagonal elements reside on the same side as the diagonal.

For the comparative model, we identified and compared two peptides that possess similar chemical and biological profiles in binding and activity at the δ opioid receptor. DPDPE was compared and contrasted with its reduced analog, acyclic DPDPE, because of their similar radioligand binding affinity ratios (MVD/GPI: DPDPE = 162, acyclic DPDPE = 114) (Yamamura and Malat, personal communication) as well as similar biological potencies (MVD/GPI: DPDPE = 3164, acyclic DPDPE = 482. δ IC_{50}): DPDPE = 1.8 nM, acyclic DPDPE = 4 nM) (Kramer, Davis, Misicka, and Hruby, personal communication). Due to the structural similarity of DPDPE and acyclic DPDPE, we felt that their conformations and topography must be similar at the δ receptor site to elicit such comparable binding and transduction profiles. However, the acyclic analog contains two polar thiol groups relative to the disulfide in the cyclic analog. It is possible that the acyclic DPDPE would be more hydrophilic than DPDPE and the less permeable of the two through bilayer membranes. This hypothesis is based on the theory that hydrophobicity correlates with permeability. Surprisingly, in permeability studies with model zwitterionic bilayer membranes, Ramaswami et al. (1992) found just the opposite to be the case: acyclic DPDPE was, in fact, approximately 4 times more permeable than DPDPE. Since the only major difference between DPDPE and acyclic DPDPE is the increased conformational flexibility of the latter, we decided to address two hypotheses: (1) a highly folded solution phase conformation of acyclic DPDPE was responsible for increased membrane permeability; (2) a permeability facilitating conformational change occured at the membrane interface. Neither of these conformational states are available to cyclic DPDPE. Here, we address the question as to whether or not conformational changes occur on binding to the membrane surface compared to the solution structure. We report the TRNOE studies of DPDPE and its reduced counterpart, acyclic DPDPE (Figure 1).

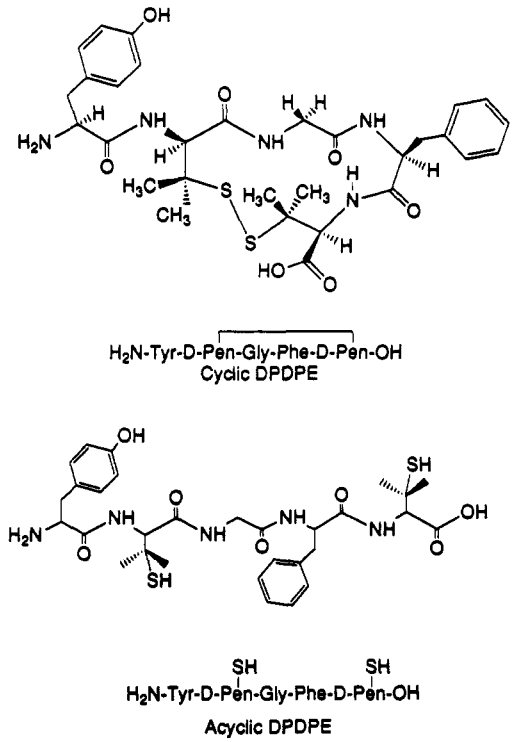

FIGURE 1: Structures of cyclic [D-Pen^2, D-Pen^5]-enkephalin (DPDPE) and acyclic [D-Pen^2, D-Pen^5]-enkephalin (acyclic DPDPE).

MATERIALS AND METHODS

Peptide Synthesis. DPDPE was purchased from Multiple Peptide Systems (San Diego, CA) as part of the National Institute on Drug Abuse program project grant.

Acyclic DPDPE was synthesized via solid phase methodology using 1% cross-linked chloromethylated polystyrene (Merrifield) resin (Peptides International, Louisville, Kentucky). The Boc-*S*-paramethylbenzyl-D-penicillamine was coupled to the resin via the method of Gisin (1973). Substitution was 0.5 mequiv g^{-1}. Couplings were achieved using 2 equiv of the appropriately protected amino acid, 2 equiv of benzotriazol-1-yltris(dimethylamino)phosphonium hexafluorophosphate (BOP) reagent, 2 equiv of diisopropylethylamine, 2 equiv of hydroxybenzotriazole, and *N*-methylpyrrolidinone as solvent. Couplings were monitored by the method of Kaiser (1970). Deprotection was achieved by using 40% trifluoroacetic acid in methylene chloride and 2% anisole followed by washing with methylene chloride, neutralizing with 10% diisopropylethylamine in methylene chloride, and a final rinsing with methylene chloride. Peptides were cleaved from the resin by adding hydrogen fluoride (HF) (10 mL/g of resin) and 10% anisole and stirring at 0 °C for 1 h. HF was then removed in vacuo to leave a flocculent white residue.

HPLC Purification and Mass Spectrometry Analysis. High-pressure liquid chromatography was conducted on a Perkin-Elmer 410 BIO LC pump equipped with a Perkin-Elmer LC-235 diode array detector and GP-100 graphics printer. Peptides were monitored at dual wavelengths of UV_{A280} and UV_{A225}. The product was dissolved in 0.1% aqueous trifluoroacetic acid (TFA), filtered through a 0.22-μm filter, and purified by HPLC using a Vydac TP1010 reverse phase column. Peptides were isolated using a solvent system consisting of 10% acetonitrile (Burdick and Jackson, HPLC

Table I: Calculated DMPC-d_{54} Unilamellar Membrane Diameters from Quasielastic Light Scattering Measurements at 60, 90, and 120° As Determined by the Deconvolution Method of CUMULANTS[a]

	60°	90°	120°
DMPC-d_{54}	102.8 ± 3.4	94.4 ± 2.0	97.7 ± 7.5

[a] A minimum of three measurements were taken at each angle and the final values were attained as the average of all measurements. Average of all measurements: 98.2 ± 5.9 nm.

grade): 90% aqueous TFA (0.1%) and enriching with a linear gradient to 40% acetonitrile: 60% TFA (0.1%) over 30 min.

The HPLC profile of acyclic DPDPE was compared to the product obtained from the reduction of DPDPE in the presence of dithiothreitol (Biorad). They were found to be identical.

Acyclic DPDPE characterized by fast atom bombardment mass spectrometry at the Mass Spectrometry facility in the School of Pharmacy at the University of Arizona. The vehicle was a glycerol matrix. The calculated mass (m/z) for the acyclic DPDPE analog was 637.8 and the actual mass observed was 638.

Liposome Preparation. 1,2-Dimyristoyl-3-*sn*-glycerophosphatidylcholine-d_{54} (DMPC-d_{54}) was purchased from Avanti Polar lipids. Nuclepore filter membranes were purchased from VWR Scientific Company (Phoenix, AZ). Sodium phosphate buffer, 12 mM, pH = 7.4, from Milli-Q water was filtered through 0.22-μm filters prior to use.

A DMPC-d_{54} chloroform solution was dried in vacuo for 6 h. The dried and weighed lipid film was then hydrated at room temperature with sodium phosphate buffer to give a concentration of 10 mg mL^{-1}. This was followed by sonication in a bath type sonicator for 1 min to produce a uniform suspension. Extended bilayers were formed by taking the lipid through 10 freeze–thaw cycles. The bilayers were extruded 10 times through 0.1-μm Nuclepore membranes at a constant pressure of 300 psi at 40 °C in a stainless steel extruder (Lipex Biomembranes, Inc.) (Hope et al., 1986).

Quasielastic Light Scattering. The diameter of the extruded liposomes were determined by quasielastic light scattering (Kolchens et al., 1992). All measurements were made with a Brookhaven Instruments' laser light scattering system consisting of a 5-mW vertically polarized helium–neon laser as a light source and a BI-200SM multiangle goniometer interfaced to a BI-8000AT digital autocorrelator. Typically, a 25-μL aliquot was diluted with prefiltered sodium phosphate buffer until a sampling rate of 50 kHz at 90 °C was achieved. The sample was repeatedly filtered through a 0.8-μm filter, until scattering due to the residual dust was eliminated. Measurements were made at 60, 90, and 120 °C until the total counts were in the range of 10^6–10^7 with 15 nonlinearly spaced channels. At least three measurements were made at each angle and the data were deconvoluted by the methods of CUMULANTS (Koppel, 1972), exponential sampling (Osterowsky & Sornette, 1989), NNLS, and CONTIN (Provencher, 1976, 1982a, 1982b).

Table I lists the calculated liposome diameters derived from measurements at each angle.

Viscosity Studies. The viscosity of the peptide solution (DPDPE) in buffer in the absence and in the presence of liposomes was determined relative to that of the buffer. All experiments were carried out in a Canon–Fenske viscometer with a bore size of 50 (viscosity range 0.4–4 centistokes). Inherent viscosities were determined at a peptide concentration of 0.5 g dL^{-1} at 30 ± 1.0 °C. The relative viscosity η_{inh} was determined using the ratio

$$\eta_{rel} = t_s/t_o$$

where t_o = solvent efflux in seconds and t_s = solution efflux in seconds.

Table II: Relative and Inherent Viscosities for DPDPE in the Presence and Absence of DMPC Membranes

peptide:lipid	efflux time (s)	η_{rel}	$\eta_{inh} = \ln[(\eta_{rel}/g)/dl]$
buffer	217.6 ± 0.1	1.00	
6.6 mM DPDPE only	222.5 ± 0.4	1.02	0.713
22:1	223.7 ± 0.6	1.03	0.733
11:1	222.3 ● 1.8	1.02	0.733
7.4:1	222.3 ● 1.0	1.02	0.733

The inherent viscosity was calculated using the following relationship:

$$\eta_{inh}\ (g\ dL^{-1}) = \ln[\eta_{rel}/[peptide]]\ (g\ dL^{-1})$$

The solvent efflux time was first measured in a constant temperature bath set at 39 ± 1 °C followed by the peptide: buffer solution (6.6 mM peptide). Finally, lipid was added to a minimum peptide:lipid ratio of 7.4:1. Table II lists our findings.

Sample Preparation for NMR Measurements. All samples were twice exchanged for the Cl^- salt by previously dissolving the peptides in 0.1N HCl followed by lyophilization. The lyophilized peptides were then dissolved in 12 mM phosphate buffer at pH = 7.4 to a final peptide concentration of 15 mM. Wilmad 545pp NMR tubes were previously soaked in HNO_3–H_2SO_4 (1:1, v/v) and washed thoroughly with distilled, deionized water. D_2O (10%) (Aldrich, low paramagnetic, T_1 = 48.1 s) was used as a lock solvent for the NMR. In addition, 0.5 mM dithiothreitol (Biorad) was added, in some cases, to the acyclic DPDPE to maintain the molecule in the reduced, acyclic form. For transferred NOE studies, the peptide: liposome ratios were varied from a maximum of 15:1 to an optimal ratio of 3:2.

NMR Data. All samples were run on a Bruker AM-500 NMR spectrometer with a variable temperature probe and interfaced to an Aspect 3000 computer. All data handling was performed on a Silicon Graphics 4D/20G or 4DG/35+ and processed with the FELIX 1.1 and 2.0 software graciously provided by Dr. Dennis Hare (Hare Research Inc., Woodinville, Wa.). All 1-D spectra were run with a sweep width of 6024 Hz and digitized with 32K complex points to provide a digital resolution of 0.4 Hz/pt. Solvent suppression was achieved by presaturation of the water proton resonance. T_2 relaxation experiments were conducted using the Meiboom–Gill modification of the Carr–Purcell spin-echo pulse sequence (Carr & Purcell, 1954; Meiboom & Gill, 1958). For the free ligand, 40 τ values were incorporated ranging from 4 ms to 1.2 s while for the bound ligand, 30 τ values were used ranging from 2 to 300 ms. All T_2 determinations were fitted to the equation:

$$A = A_0 e^{-\tau/T_2}$$

using the DISNMR software provided by Bruker Instruments.

Determination of the correlation time τ_c was based upon the rate equation for the intramolecular contribution to relaxation according to the equation given by

$$\frac{1}{T_{2\ intra}} = \frac{2\gamma^4 h^2 I(I+1)}{5r^6}\left[\frac{\tau_c}{1+\omega^2\tau_c^2} + \frac{4\tau_c}{1+4\omega^2\tau_c^2}\right]$$

(Abragam, 1961). Calculation of correlation time τ_c assumed

an average distance between the geminal methyl protons of 1.8 Å and that the methyl protons comprised the predominant mode of relaxation. Correlation times were determined using the Mathplot software program.

All 2-D experiments were conducted utilizing 6024-Hz sweep width and digitized with 2K complex points to give a digital resolution of 6 Hz/pt. A 2-s relaxation delay for reequilibration was utilized between pulses. Routinely, two dummy scans were used followed by 32–64 scans. A total of 400–800 real points were collected along t_1. The 90° pulse width was determined to be 6.8 μs. All spectra were referenced relative to the HOD resonance at 4.76 ppm.

Two-dimensional double quantum filtered COSY (DQF COSY) experiments were acquired with standard pulse sequences and phase cycling (Rance et al., 1983). Two dimensional nuclear Overhauser effect (NOE) spectra (Jeener et al., 1979; Kumar et al., 1980) were acquired in the pure absorption mode (Redfield & Kuntz, 1975) using the time proportional phase incrementation method along t_1 (Marion & Wüthrich, 1983; Bodenhausen et al., 1984). For the free ligand, mixing times ranged from 100 ms to 1 s. Cross peak intensities were maximized at a τ_m of 800 ms and little to no NOE development was observable at mixing times less than 200 ms. In addition, all cross-peak intensities were in the positive limit. Membranes were then added until, empirically, a sufficient amount of line broadening of the 1D spectrum was observed. Optimally, a ratio of 3:2 (ligand:membrane) was used. Two-dimensional NOESY spectra were then run using a mixing time of τ_m = 50–100 ms to allow for rapid cross-relaxation. The observed spectra were now significant for the fact that all off-diagonal elements were in the negative NOE limit (same side as the diagonal elements).

Molecular Modeling. Neutral non-zwitterionic starting structures for minimization were produced interactively using the modeling package MacroModel (Mohamadi et al. 1990) on a Silicon Graphics 4DG/35+ Workstation. Using the option MULTIC, a systematic grid search of the backbone ϕ and ψ dihedrals was performed such that each dihedral was incremented through 60° steps (i.e. six per torsion). Side chain dihedrals were similarly considered but with 120° increments corresponding to the ± gauche and trans orientations. During the search, combinations of angles that produced conformations with high-energy steric interactions were rejected. In addition the search was biased to find only structures that were compatible with the NMR data by inclusion of distance constraints determined from the NOE profiles. Semiquantitative NOE constraints were applied using the following distance bounds: strong (1.5–2.5 Å); medium (2.5–3.5 Å); weak (3.5–4.5 Å). Structures not satisfying these interproton distance bounds were also rejected.

Located starting structures were energy minimized on a Convex C220 using BATCHMIN (Mohamadi et al. 1990). All structures were minimized in the AMBER force field with a dielectric constant of 10.0 to reduce over estimation of electrostatic interactions in these vacuum phase calculations. Semiquantitative NOE interproton distance restraints which were used to locate the starting structures were applied during minimization to favor the location of low-energy conformers consistent with the NMR data. Initial refinement was achieved using the conjugate gradient minimizer followed by exhaustive minimization with the block-diagonal Newton Raphson procedure to produce all low energy conformers with an RMSD < 0.1 kJ/(mol Å). At each stage of energy minimization all structures were compared by RMS overlay of the C_α and C_β carbons and duplicate structures (as indicated by RMS < 1.0 Å^2) were rejected.

Table III: ^{1}H NMR Assignments of (A) [D-Pen^2,D-Pen^5]-Enkephalin (DPDPE) and (B) Acyclic [D-Pen^2,D-Pen^5]-Enkephalin in 90% H_2O/10% D_2O Phosphate Buffer, pH = 7.4[a]

	DPDPE	acyclic DPDPE
Tyr^1		
NH	NO	NO
CH_α	4.36	4.34
CH_β	3.04, 3.16	3.06, 3.16
arom	6.84, 7.18	6.83, 7.14
D-Pen^2		
NH	8.24	8.21
CH_α	4.18	4.18
methyl	0.81, 1.46	1.24, 1.09
Gly^3		
NH	8.55	8.48
CH_α	3.54, 4.34	3.80, 3.87
Phe^4		
NH	8.48	7.98
CH_α	4.49	4.76
CH_β	2.97, 3.11	3.01, 3.10
arom	7.17, 7.23, 7.27, 7.29, 7.31	7.20, 7.22, 7.26, 7.31, 7.33
D-Pen^5		
NH	7.38	7.61
CH_α	4.37	4.17
methyl	1.29, 1.34	1.18, 1.34

[a] Assignments are based upon referencing to the HOD peak in the spectrum equal to 4.76 ppm. [b] NO = not observed.

RESULTS AND DISCUSSION

Spectral assignments of proton resonances were obtained by the sequential resonance assignment method (Wagner et al., 1981; Billeter et al., 1982). Table III lists the chemical shift assignments for DPDPE and the acyclic DPDPE. The assignments for DPDPE were consistent with those previously reported (Hruby et al., 1988).

Although the data are not shown, DPDPE exhibited a transferred NOE with DMPC-d_{54} membranes. A detailed comparison of the free and membrane-bound NOE profiles of DPDPE at 500 MHz would have been desirable. Unfortunately, however, as will be explained in detail later in this section, the free DPDPE resided too close to the zero NOE limit in solution at 500 MHz to make this comparison possible. Hence, the membrane-bound NOE profile acquired at 500 MHz was compared to the free DPDPE NOE profile previously performed at 250 MHz (Hruby et al., 1988). As might be expected for a peptide with such a constrained cyclic structure, very little change was observed in the NOE patterns of the backbone ring conformation of the membrane bound spectrum vs. the free ligand profiles performed previously (Hruby et al., 1988). As a matter of fact, the only change in the backbone NOE profile was the addition of a weak intraresidue α-NH interaction of the Phe^4 in the bound state (see Figure 6). Because the NOE profiles of free and bound DPDPE were so similar in number as well as their intensities, this indicated that the backbone of these two forms still maintained the same conformations. With regards to the side-chain topography, we did note some differences in intensities of the Tyr^1 and Phe^4 NOEs between α and β protons which may reflect a change in rotamer populations upon interaction with the membrane. However, the evidence indicated that interaction with the membrane surface did little to modify the overall conformation of DPDPE compared to its aqueous solution structure.

Conversely, the interaction of acyclic DPDPE with DMPC-d_{54} membranes showed striking differences between its bound

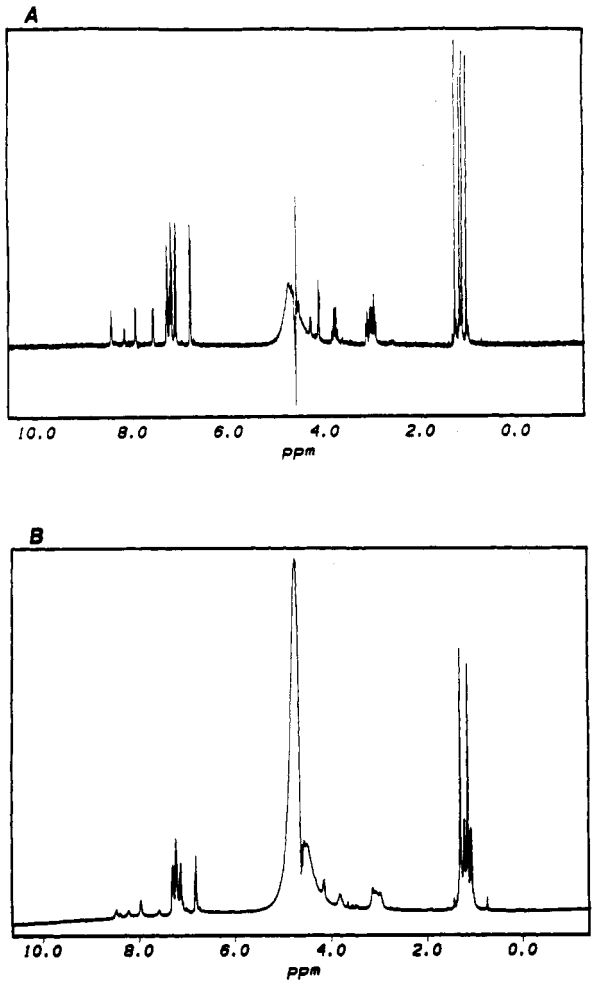

FIGURE 2: 500-MHz ^{1}H NMR of the methyl region of 15 mM acyclic DPDPE in 12 mM phosphate buffer: (A) acyclic DPDPE ligand in solution in the absence of 10 mM DMPC-d_{54} membranes; (B) acyclic DPDPE in the presence of 10 mM DMPC-d_{54} membranes. Note the significant line broadening which occurs as a function of exchange processes with the membrane.

ligand NOE profile compared to the bound ligand NOE profile of cyclic DPDPE. Figure 2 displays the 1D spectrum of the free-ligand of the acyclic DPDPE *vs.* the ligand-membrane solutions at 39 °C. There was a significant amount of line broadening in the case of the membrane-bound ligand as compared to the free ligand. This indicated that the ligand also exhibited exchange processes between the solution and the membrane.

Figure 3 displays the amide region of the 2D NOESY spectra of acyclic DPDPE in both the (A) absence of DMPC-d_{54} membranes and in the (B) presence of 10 mM DMPC-d_{54} membranes. Clearly, the free ligand resides in the positive NOE limit whereas the bound ligand in the presence of membranes resides in the negative limit. Dithiothreitol (DTT) was also used as an internal control for determination of viscosity effects upon the line broadening of the resonances. The data (not shown) revealed a significant broadening of the peptide resonances in the presence of the membrane vesicles but no significant broadening of the DTT resonances was observed. This indicated that the NOE spectrum in the presence of membranes reflected an exchange process and was not due to viscosity.

Viscosity measurements were conducted to rule out this possibility. Table II lists the results for different peptide–membrane mixtures. The addition of peptide to buffer increased the viscosity of the solution slightly; however, this

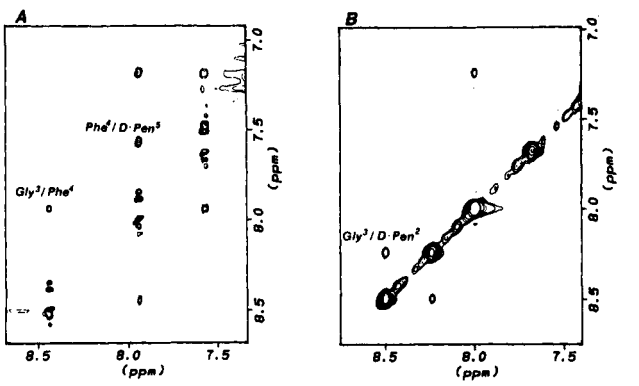

FIGURE 3: 500-MHz ^{1}H 2D NOESY spectra (tppi mode) of the amide region of acyclic DPDPE: (A) acyclic DPDPE in the absence of DMPC-d_{54} membranes (note the absence of diagonal elements); (B) acyclic DPDPE in the presence of 10 mM DMPC-d_{54} membranes (note the presence of diagonal elements). Note the presence of the D-Pen^2 NH connectivity to the Gly^3 amide which is absent in the NOESY spectrum of the free ligand without membranes present. In contrast, note also the presence of the Gly^3–Phe^4 and Phe^4–D-Pen^5 NH–NH dipolar coupling in part A which is absent in the bound ligand part (B).

was not a concern because all NOESY spectra of the free ligand resided in the positive NOE limit. More importantly, the viscosity in the presence of added membranes up to a peptide:lipid ratio of 7.4:1 was virtually identical to that of the peptide–buffer solution. Unfortunately, further viscosity studies at higher lipid ratios were complicated by bubble formation in the suspension, thus making determinations through the microbore Canon Fenske viscometer difficult and unreliable. Nonetheless, the data indicated viscosity was not a factor in the NOESY spectra since transferred NOEs were observed even with peptide:lipid ratios as high as 15:1.

Figure 4 shows the methyl region of the D-Pen^2 and D-Pen^5 β,β-dimethyls. Note the large difference in line broadening between the D-Pen^2 and D-Pen^5 methyls caused by the addition of membrane vesicles. The greater line broadening of the D-Pen^2 β,β dimethyls *vs.* the D-Pen^5 β,β dimethyls indicated the stronger interaction of the D-Pen^2 moiety with DMPC-d_{54} membranes compared to the D-Pen^5 moiety. Thus, the D-Pen^2 side chains were in a more "rigid" environment. This observation was consistent with the D-Pen^2 moiety interacting with the zwitterionic membrane surface more than the D-Pen^5. This indicated that the peptide did not interact with the membrane surface in a random fashion, but rather, that the N-terminus provided a favorable electrostatic interaction with the membrane surface. Epand and co-workers (Epand et al., 1988) demonstrated the importance of peptide charge on peptide–lipid interactions by the observed greater interaction of cationic Arg^4 pentagastrin with lipid membranes than the corresponding anionic pentagastrin. Our observation was also in agreement with proposals by Jarrell and coworkers (Jarrell et al., 1980) who suggested that the amine terminal charge was responsible for directed interactions with phospholipids. In addition, the differential line broadening of the D-Pen^2 could reflect the initial insertion of the amine terminus into the membrane. Figure 5 displays the membrane-bound 2D NOESY NH (F2), α, β, γ (F1) region.

T_2 measurements conducted on the methyl region verify that the differential line broadening between the D-Pen^2 and D-Pen^5 side chains indeed reflect a difference in the rate at which these methyl groups relax. It is noted that the free-ligand methyl resonances exhibited T_2 values of similar times (55–67 ms) whereas the membrane-bound ligand exhibited differences between the D-Pen^2 methyls (8 and 9 ms) and the

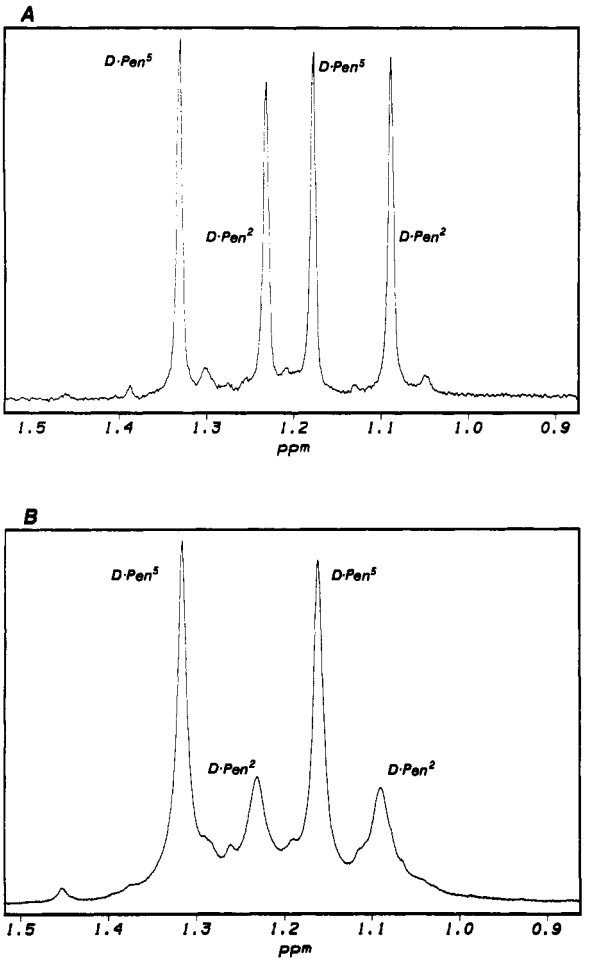

FIGURE 4: 500-MHz ^{1}H 1D NMR spectra of the β,β-dimethyl resonances of D-Pen^2 and D-Pen^5 of the acyclic DPDPE: (A) ligand in 12 mM phosphate buffer, pH = 7.4; (B) ligand in the presence of 10 mM DMPC-d_{54} membranes (membrane size = 98.2 ± 5.9 nm). Note in part B the greater extent of line broadening for the D-Pen^2 methyls *vs.* the D-Pen^5 methyls, indicating a closer proximity of the D-Pen^2 methyls to the membrane surface.

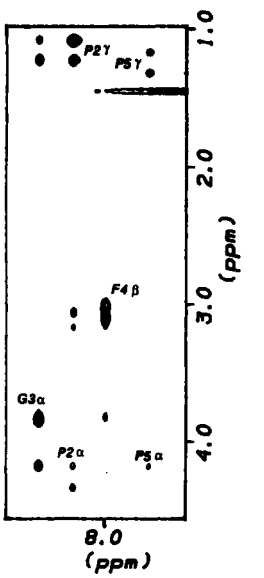

FIGURE 5: 500-MHz spectra of the NH (F2), α, β, γ (F1) region of 15 mM acyclic DPDPE in the absence (A) and presence (B) of 10 mM DMPC-d_{54} membranes. The spectrum in part A of the "free" ligand employed a τ_m of 800 ms while the spectrum in part B of the "bound" ligand employed a τ_m of 100 ms to account for the difference in cross-relaxation rate for the ligand in the presence and absence of membranes respectively. Note qualitatively the difference in profiles.

Table IV: Spin–Spin Relaxation (T_2) Values for the D-Pen^2 and D-Pen^5 Methyl Protons in the Presence and Absence of DMPC-d_{54} Bilayer Membranes As Measured at 500 MHz Using a Standard Carr–Purcell–Meiboom–Gill Pulse Sequence

residue	δ (ppm)	T_2(free) (ms)	T_2(bound) (ms)
D-Pen^2	1.24	68	9
D-Pen^2	1.09	56	9
D-Pen^5	1.34	67	19
D-Pen^5	1.18	62	18

D-Pen^5 methyls (18 and 19 ms) respectively. Table IV lists the relaxation values. Calculation of rotational correlation times using the T_2 data for both free and membrane-bound ligands revealed that the free ligand in solution exhibited a correlation time τ_c of approximately 0.21 ns. We also calculated the τ_c corresponding to the zero NOE limit as being approximately 0.36 ns. Although the free ligand resided in the positive NOE regime, it was clear that the NOE intensities would be unreliable for modeling purposes because they were so close to the zero NOE limit. The same was also true for the free form of DPDPE. On the other hand, the membrane-bound acyclic DPDPE possessed a correlation time of 4.6 ns, placing it well into the negative NOE regime. Because the NOE intensities for the free ligands were uniformly weak, we concluded that only the NOE profiles of the membrane bound conformers were reliable enough to perform further modeling studies.

Extensive molecular modeling of cyclic DPDPE had been performed previously (Froimowitz & Hruby, 1988; Hruby et al., 1988; Mosberg et al., 1990; Pettitt et al., 1991; Wilkes & Schiller, 1991). DPDPE in solution assumes an amphiphilic structure whereby the backbone formed the hydrophilic face and the side-chain aromatic moieties formed the hydrophobic face. Our current NMR data profile was completely consistent with these previous findings, and so it was unnecessary to remodel this conformation here. Suffice it to say that previous modeling in both the vacuum phase (Hruby et al., 1988) and in the presence of explicit water molecules (Pettitt et al., 1991), revealed almost identical conformations and topographies (see Figure 7). Compared to previous NOE profiles of cyclic DPDPE in solution (Hruby et al., 1988), the membrane-bound form of cyclic DPDPE changed little if at all. Hence we concluded that the free and membrane bound forms represented the same conformation.

Since no conformations have been reported for acyclic DPDPE, we would have liked to model the solution and membrane bound conformations in detail. However, the solution phase T_2 analysis of the methyl protons of the D-Pen residues indicated a τ_c value corresponding to the near zero NOE intensity limit. Hence, despite the relatively large number of NOEs observed in the free state (Figure 6) the dipolar intensities were of questionable reliability and thus could not be used as accurate constraints in modeling. In contrast, in the TRNOE experiment, the correlation time for acyclic DPDPE in the bound state was significantly larger. Thus, the NOE intensities were much more intense as well. Surprisingly, for the membrane bound structure relatively few NOEs were observed compared to experiments in the absence of liposomes (Figure 6). The fact that rather few NOEs were observed was viewed as conformationally significant and indicated a rather specific peptide structure at the membrane surface.

Putative membrane-bound conformations were generated in a systematic search of the torsion angles of acyclic DPDPE, using the transfered NOEs as constraints to limit the search

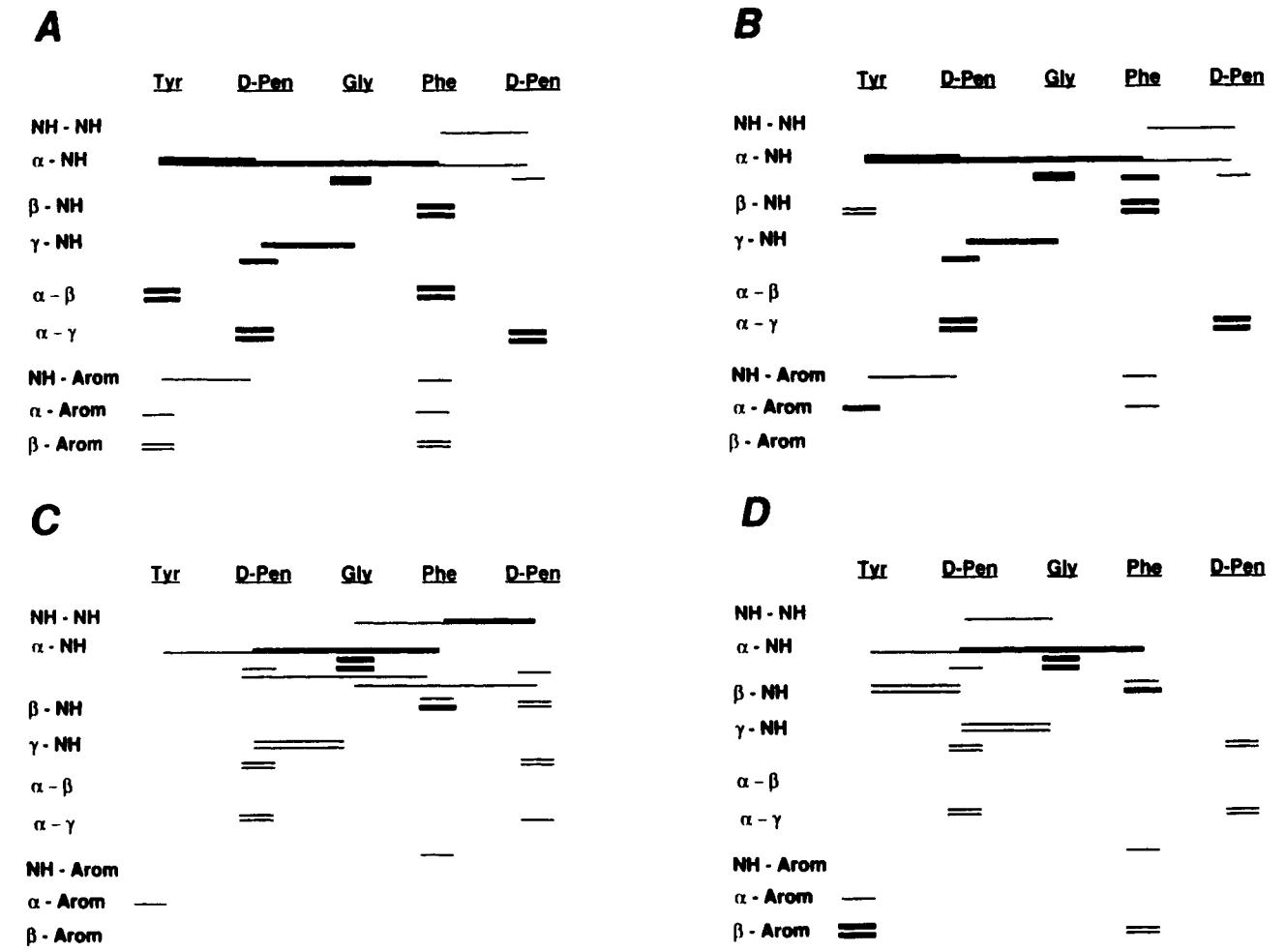

FIGURE 6: NOE profile of 15 mM DPDPE (A) and 15 mM acyclic DPDPE (B) in the presence of 10 mM DMPC-d_{54} membranes. NOEs are arranged in terms of strong (thick bars), medium (medium thickness), and weak (thin bars) intensities using the criteria of Williamson and co-workers (1985).

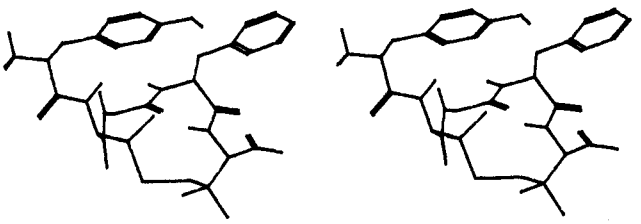

FIGURE 7: Stereoview solution phase structure of cyclic [D-Pen^2, D-Pen^5]-enkephalin (DPDPE) modeled in the presence of 421 explicit water. Waters have been removed for clarity. Note the amphiphilic nature of the molecule situating the hydrophobic sidechains on one face and the hydrophilic backbone on the opposite face. Reproduced with permission from Pettitt et al. (1991). Copyright 1991 Rockefeller University Press.

to those structures consistent with experiment observation. Restrained energy minimization thus produced a set of low-energy conformations which were considered as representing the ensemble of NMR structures at the membrane surface. All were assumed to be important and the structure set was examined entirely for major conformational similarities and differences.

Using the method of Lewis et al. (1973), the population of β-turns in acyclic DPDPE over the total number of conformations found was assessed by measuring all $C\alpha_i - C\alpha_{i+3}$ interatomic distances. Those less than 7.0 Å apart were assumed to form a reverse turn about the $i + 1$ and $i + 2$ residues (Table V). Unsurprisingly, the most populated turns were found around the D residues in positions 2 and 5. A turn

Table V: Percentage of β-Turn Populations of All Possible Turns in Acyclic DPDPE[a]

residues in β-turn	conformation set	
	% free solution	% membrane-bound
D-Pen^2–Gly^3	50	91
Gly^3–Phe^4	5	66
Phe^4–D-Pen^5	31	34

[a] Percentages were calculated as % population = no. of turns around $xaa_{i+1} - Yaa_{i+2}$/total no. of conformations in the NMR ensemble, where, the number of conformations in the NMR ensembles found by modeling were (A) free solution = 42 and (B) membrane-bound = 80. Note that more than one turn may be found in each conformation. Thus, the percentage populations are independent of one another (i.e. the sum of the percentages does not equal 100%). Turns were identified by the method of Lewis et al. (1973).

about D-Pen^2–Gly^3 was found to be approximately 91% populated in membrane bound structures (Figure 8; Table V). A bend about Gly^3–Phe^4 was also significantly populated (66% populated) and a gradual decline in turn structure is observed in moving from the N to the C terminus (34% turn population at the C-terminal dipeptide). This may be consistent with the N terminal being embedded in the membrane surface and acting as a nucleation site upon which the rest of the peptide may be folding in an α-helical manner. The C terminal is thus less constrained by the membrane surface and exhibits more structural disorder. However no purely α-helical conformations were observed in the membrane bound ensemble, and it is unlikely that such a short peptide

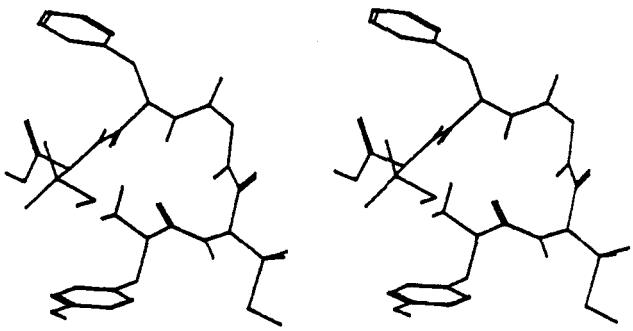

FIGURE 8: Stereoview of a low-energy conformation found for acyclic DPDPE in the presence of DMPC-d_{54} bilayer membranes. Note the extended arrangement of the side chains in the membrane-bound form compared to cyclic DPDPE (Figure 7).

could fold into a stable helix. These results may demonstrate the initial folding stages of a stable α-helix that would be observed in longer peptides (Erne et al., 1985)

Interestingly, compared to DPDPE, our modeling results for acyclic DPDPE revealed an entirely different scenario. While a β-turn was constrained about Gly^3–Phe^4 by the disuflide bridge formed between the D-Pen^2 and D-Pen^5 in cyclic DPDPE (Figure 7), a highly populated β-turn about D-Pen^2 and Gly^3 was located the membrane bound conformer. However, while the solution phase and membrane bound conformations for cyclic DPPDE favored close interaction or overlapping of the Tyr^1 and Phe^4 aromatics to minimize hydrophobic contact with solvent (Figure 7), these side chains were well separated on either side of the D-Pen^2-Gly^3 reverse turn in the membrane bound structures of acyclic DPDPE (Figure 8). In addition, we also observed that the Phe^4 and D-Pen^5 of the acyclic form now assumed a more extended conformation which forces the sidechains to point away from one another.

When considered with the experimental observations, it was notable that the membrane-bound structure was effectively divided into two sections separated on either side of the D-Pen^2–Gly^3 reverse turn. In the presence of the membrane, the Tyr^1–D-Pen^2 region appeared to preferentially interact with the surface of the membrane as indicated by the differentially increased line broadening observed for the protons in these residues in the presence of liposomes. However the Gly^3–Phe^4–D-Pen^5 region on the other side of the turn extended into the aqueous milieu, thus making the carboxyl end more conformationally flexible. This indeed appeared to account for the Tyr^1 side chain being directed into the membrane and the Phe^4 side chain initially being directed away.

CONCLUSIONS

TRNOE spectroscopy allows one to acquire information regarding the ligand bound conformation of a peptide or other ligand molecule with an acceptor molecule or supramolecular surface. Recent works focused on peptide conformations bound to lipid membranes, enzymes or carrier proteins (Hallenga et al., 1988; Bushweller & Bartlett, 1991; Landry & Gierasch, 1991, Wakamatsu et al., 1992) as well as DNA oligomers bound to DNA binding proteins (Clore et al., 1986). In contrast, little work has been reported in relation to the TRNOE method and its study with regards to peptide–membrane interactions (Milon et al., 1990). In addition, to date, we know of no published studies that address the question of conformational effects of peptides in relation to membrane permeability.

Previous work by Milon and co-workers, using enkephalin analogs and mixed DOPS/DOPC membranes, were conducted at pH's which varied between pH = 3.6–4.5 (Milon et al., 1990); their rationale being to resolve all ^{1}H resonances in the spectrum so quantitative NOE data could be observed. However, because the pK_a for the phosphoryl group of the lipid lies within this pH range, we felt that it would be more suitable to use a higher pH (pH = 7.4) in our studies so as to better reflect biological systems. In addition, Milon and co-workers found it necessary to add negatively charged phospholipids (phosphatidylserine) into the vesicles and to maintain a low ionic strength, suggesting that enkephalins interact only weakly with neutral membranes. Using our acyclic DPDPE, we found that neutral membranes in buffered phosphate solution did not pose a significant problem. We did, however, find that the NOE intensities of DPDPE were smaller than the acyclic analogue, indicating a relatively diminished interaction with the membrane.

Incorporation of these experimental parameters into computer aided molecular modeling of acyclic DPDPE indicated that the amino terminal residues Tyr^1 and D-Pen^2 were interacting with the head group region of the membrane in the bound state while the C-terminal residues Phe^4–D-Pen^5 lie close to the surface of the membrane but, in contrast to the amino terminal, are projecting into the bulk solution (see Figure 8). This was consistent with the larger line broadening for the D-Pen^2 methyls as opposed to the D-Pen^5 methyls. Cyclic DPDPE cannot adopt the proposed bound conformation and therefore must interact with the membrane in a different manner. Given the relatively rigid amphiphilic nature of DPDPE (Hruby et al., 1988) in solution and at the membrane surface, this cyclic peptide may bind to liposomes either through hydrophobic interactions of the aromatic residues or via electrostatic contacts of the peptide amine and carboxyl termini with the phosphatidylcholine head group. Since our results indicated that both charge–charge as well as hydrogen-bonding contacts were important, the latter model for cyclic DPDPE binding seemed most likely. This was consistent with the uniform line broadening observed for the proton resonances of the cyclic peptide in the presence of membranes compared to those of acyclic DPDPE.

If this electrostatic mode of binding was important in DPDPE then the decreased interaction of the cyclic peptide may be due to the close proximity of the amine and carboxy termini forming a salt bridge. This would effectively decrease the overall charge on the molecule and so reduce electrostatic interaction with the membrane. The formation of a salt bridge in DPDPE had been observed as a stable conformation in molecular dynamics simulations in water (Pettitt et al., 1991).

The fact that DPDPE and its acyclic analogue exhibit different binding modes was also suggested by differential scanning calorimetry studies (Ramaswami et al., 1992). The main phase transition (T_m) of DPPC membranes in phosphate buffer was unaffected by DPDPE whereas the acyclic DPDPE did exhibit a small but significant effect on the T_m. A more striking effect, with regard to the current studies, was the elimination of the pretransition at 34 °C by the acyclic DPDPE, but not the cyclic peptide. Jacobs and White (1986) reported that addition of certain hydrophobic tripeptides to DMPC bilayers abolishes the pretransition, while only broadening the main transition. The pretransition was associated with a change in lipid chain tilt relative to the head groups as is a consequence of the surface area requirements of the polar head groups. In contrast, DPDPE was weakly bound to the bilayer surface without actually altering the ordering of the head group region, and thus little effect on the pretransition occured.

The current work made two key comparisons: (1) a comparison of the possible conformational differences of opioid peptides between the solution phase and the membrane bound phase and (2) an examination of the conformational differences in the bound states *between* two peptides of similar structure and biological profiles, differing primarily by a conformational constraint. Clearly, we could see that the acyclic DPDPE exhibited an entirely different NOE profile upon interaction with the membrane surface, than its cyclic counterpart, DPDPE. Ramaswami et al. (1992) showed that the acyclic DPDPE permeated through POPC/POPE/cholesterol bilayer membranes significantly faster than DPDPE. Because it was apparent from the TRNOE experiments that acyclic DPDPE could undergo more conformational changes than its cyclic counterpart, we concluded that our results are consistent with the hypothesis that increased permeability was correlated to the peptides ability to undergo conformational changes at the membrane surface. Hence, by virtue of greater flexibility, acyclic DPDPE was able to adapt and permeate through the changing membrane environment (i.e. from solution to polar head group to lipid bilayer etc.) more readily than the cyclic counterpart.

The TRNOE data suggested some possibilities concerning the nature of the interaction of the peptide with the membrane surface. Acyclic DPDPE, although containing more polar components, may be able to "effectively" mask its polarity via a conformational change at the membrane surface, thus rendering the molecule more permeable than DPDPE. This suggests that the acyclic molecule is more able to accomodate to a nonaqueous environment. Alternatively, the acyclic DPDPE, upon conformational change, may be able to rid itself of waters of hydration, thus requiring less free energy to permeate through the membranes. Clearly, through TNROE and molecular modeling, we have begun to define the solution phase *vs.* membrane-bound conformations.

We undertook these studies with the intention of examining where dynamic conformational changes may affect permeability through model membranes by comparing two similar molecules that differ primarily in their conformational flexibility. Both peptides possess similar binding constants, MVD/GPI ratios, and IC_{50} values. It was clear that the acyclic DPDPE could assume the biologically relevant conformation to elicit binding and transduction at the receptor site. However, through a series of biophysical studies, it also became clear that receptor requirements may be different from permeability requirements. These observations suggested that the acyclic DPDPE free ligand could assume a conformation that was more flexible than the cyclic DPDPE, thereby interacting more at the membrane surface. The implication of the study suggested that the appropriate conformational flexibility in peptides may be an important component that must be considered when determining the factors necessary for a favorable interaction with the membrane surface which may be instrumental in determining the subsequent events that lead to permeation through the entire membrane.

ACKNOWLEDGMENT

We wish to acknowledge the help of Dr. Kenner Christenson for technical assistance regarding our NMR studies. We also wish to acknowledge Dr. Dennis Hare and Dr. Kevin Banks for graciously providing us with the FELIX software package and providing technical support.

REFERENCES

Abragram, A. (1961) *The Principles of Nuclear Magnetism*, Oxford University Press, London and New York.

Banks, W., & Kastin, A. (1985) *Brain Res. Bull. 15*, 287–292.

Billeter, M., Braun, W., & Wüthrich, K. (1982) *J. Mol. Biol. 151*, 949–961.

Bodenhausen, G., Kogler, H., & Ernst, R. R. (1984) *J. Magn. Reson. 58*, 370–388.

Bushweller, J. H., & Bartlett, P. A. (1991) *Biochemistry 30*, 8144–8151.

Carr, H. Y., & Purcell, E. M. (1954) *Phys. Rev.* 630–638.

Clore, G. M., & Gronenborn, A. M. (1982) *J. Magn. Reson. 48*, 402–417.

Clore, G. M., & Gronenborn, A. M. (1983) *J. Magn. Reson. 53*, 423–442.

Clore, G. M., Gronenborn, A. M., Greipel, J., & Maas, G. (1986) *J. Mol. Biol. 187*, 119–124.

Epand, R. M., Surewicz, W. K., & Yeagle, P. (1988) *Chem. Phys. Lipids 49*, 105–110.

Erne, D., Sargent, D. F., & Schwyzer, R. (1985) *Biochemistry 24*, 4261–4263.

Froimowitz, M., & Hruby, V. J. (1989) *Int. J. Pept. Protein Res. 34*, 88–96.

Gisin, B. F. (1973) *Helv. Chim. Acta 56*, 1476–1482.

Hallenga, K., Nirmala, N. R., Smith, D. D. & Hruby, V. J. (1988) in *Peptides: Chemistry and Biology, Proceedings of the Tenth American Peptide Symposium* (Marshall, G., Ed.) pp 468–479, ESCOM Science Publishers, Leiden, The Netherlands.

Hope, M. J., Bally, M. B., Mayer, L. D., Janoff, A. S., & Cullis, P. R. (1986) *Chem. Phys. Lipids 40*, 89–107.

Hruby, V. J. (1982) *Life Sci.* 189–199.

Hruby, V. J., & Gehrig, C. A. (1989) *Med. Res. Rev. 9*, 343–401.

Hruby, V. J., Kao, L. F., Pettitt, B. M., & Karplus, M. (1988) *J. Am. Chem. Soc. 110*, 3351–3359.

Jacobs, R. E., & White, S. H. (1986) *Biochemistry 25*, 2605–2612.

Jarrell, H. C., Deslauriers, R., McGregor, W. H., & Smith, I. C. P. (1980) *Biochemistry 19*, 385–390.

Jeener, J., Meier, B. H., Bachmann, P., & Ernst, R. R. (1981) *J. Chem. Phys. 71*, 4546–4553.

Kaiser, E., Colescott, R. L., Bossinger, C. D., & Cook, P. I. (1970) *Anal. Biochem. 34*, 595–598.

Kolchens, S., Ramaswami, V., Birgenheier, J., Nett, L., & O'Brien, D. F. (1993) *Chem. Phys. Lipids 65*, 1–10.

Koppel, D. E. (1972) *J. Chem. Phys. 57*, 4814–4820.

Landry, S. J., & Gierasch, L. M. (1991) *Biochemistry 30*, 7359–7362.

Lewis, P. N., Momany, F. A. & Scheraga, H. A. (1973) *Biochim. Biophys. Acta 303*, 211–229.

Macura, S., Huang, Y., Soter, D., & Ernst, R. R. (1981) *J. Magn. Reson. 43*, 259–281.

Marion, D., & Wüthrich, K. (1983) *Biochem. Biophys. Res. Commun. 113*, 967–974.

Meiboom, S., & Gill, D. (1958) *Rev. Sci. Instrum. 37*, 688–691.

Milon, A., Miyazawa, T., & Higashijima, T. (1990) *Biochemsitry 29*, 65–75.

Mohamadi, F., Richards, N. G. J., Guida, W. C., Liskamp, R., Lipton, M., Caufield, C., Chang, G., Hendrickson, T., & Still, W. C. (1990) *J. Comput. Chem. 11*, 4404–452.

Mosberg, H., Hurst, R., Hruby, V. J., Gee, K., Yamamura, H. I., Galligan, J. J., & Burks, T. F. (1983) *Proc. Natl. Acad. Sci. U.S.A. 80*, 5871–5874.

Mosberg, H. I., Sobczyk-Kojiro, K., Subramanian, P., Crippen, G. M., Ramalingam, K., & Woodard, R. W. (1990) *J. Am. Chem. Soc. 112*, 822–829.

Osterowsky, N., & Sornette, D. (1989) *Opt. Acta 28*, 1059–1070.

Pettitt, B. M., Matsunaga, T. O., Gehrig, C. A., Al-Obeidi, F., Hruby, V. J., & Karplus, M. (1991) *Biophys. J. 287*, 1–5.

Provencher, S. W. (1976) *J. Chem. Phys. 64*, 2772–2775.

Provencher, S. W. (1982a) *Comput. Phys. Commun. 27*, 213–227.

Provencher, S. W. (1982b) *Comput. Phys. Commun. 27*, 229–232.
Ramaswami, V., Haaseth, R., Matsunaga, T. O., Hruby, V. J., & O'Brien, D. F. (1992) *Biochim. Biophys. Acta 1109* (2), 195–202.
Rance, M., Sørensen, M., Bodenhausen, G., Wagner, G., Ernst, R. R., and Wüthrich, K. (1983) *Biochem. Biophys. Res. Commun. 117*, 479–485.
Redfield, A. G., & Kuntz, S. D. (1975) *J. Magn. Reson. 19*, 250–254.
Smith, P. E., Dang, L. X., & Pettitt, B. M. (1991) *J. Am. Chem. Soc. 113*, 67–73.
Wagner, G., Kumar, A., & Wüthrich, K. (1981) *Eur. J. Biochem. 114*, 375–384.
Wakamatsu, K., Okada, A., Miyazawa, T., Ohya, M., & Higashijima, T. (1992) *Biochemistry 31*, 5654–5660.
Weber, S. J., Greene, D. L., Sharma, S. D., Yamamura, H.-I., Kramer, T. H., Burks, T. F., Hruby, V. J., Hersh, L. D., & Davis, T. P. (1991) *J. Pharmacol. Exp. Ther. 259*, 1109–1117.
Weber, S. J., Greene, D. L., Hruby, V. J., Yamamura, H.-I., Porreca, F., & Davis, T. P. (1992) *J. Pharmacol. Exp. Ther. 263*, 1308–1316.
Weiner, J. S., Kollman, P. A., Case, D. A., Singh, U. C., Ghio, C., Alagona, G., Profeta, S., & Weiner, P. (1984) *J. Am. Chem. Soc. 106*, 765–771.
Williamson, M. P., Havel, T. F., & Wüthrich, K. (1985) *J. Mol. Biol. 182*, 295–315.